



Geometrically distributed aperiodic circular photonic crystals with broad and isotropic photonic band gaps

Qing Guo Du^{a,b}, G. Alagappan^b, H.V. Demir^a, C.H. Kam^a, X.W. Sun^{a,*}, P. Wu^b

^a School of Electrical and Electronic Engineering, Nanyang Technological University, Nanyang Avenue, Singapore 639798, Singapore

^b Institute of High Performance Computing, 1 Fusionopolis Way, #16-16 Connexis, Singapore 138632, Singapore

ARTICLE INFO

Article history:

Received 25 August 2010

Accepted 3 January 2011

Available online 14 January 2011

Keywords:

Geometrically distributed

Photonic Crystal

Photonic band gap

Broadening

ABSTRACT

In this paper, a new type of circular photonic crystal (CPC) with a geometrical distribution of concentric layers is presented. A broad and isotropic photonic band gap is achieved using this geometrically distributed CPC (GCPC). Also, the influence of the number of concentric layers to the overall band gap of GCPC is studied. It is demonstrated that the band gap broadens with a red shift when the number of concentric layers is increased. The reason for the red shift of the band gap is further investigated.

© 2011 Elsevier B.V. All rights reserved.

Photonic crystals (PCs) [1,2], which are also known as photonic band gap materials, have attracted significant attention of scientists for their applications including optical integrated circuits [3], lasers [4], high-Q cavities [5], and nonlinear optics [6]. PCs are artificial structures with alternating arrangement of various materials and form a band gap in which the propagation of electromagnetic wave is prohibited in certain range of frequencies and directions. Two dimensional PCs have been commonly periodically arranged in triangular or square lattices and the resulting band gap size obtained by these PCs has been relatively narrow and has strongly depended on the direction of the light propagation. However, some of the applications require the band gap to be broad and isotropic, which means that the band gap size needs to be invariant to changing the angle of the incident light. To date, significant research efforts have been made to broaden the bad gap. Recently a new way to construct one dimensional broad band gap PCs (called geometrically distributed one dimensional PCs) for all angles and all polarizations has been developed [7]. The whole structure contains PCs of different periods that are distributed in geometrical series with a carefully designed geometrical ratio. With a proper designation, this one dimensional geometrically distributed PC can be used to block any range of light that the designer desires to. This method can also be used to construct two dimensional, all angle broad band gap PCs.

Circular photonic crystals (CPCs) recently proposed by several groups [8,9] can be used to obtain an isotropic band gap (i.e., all directions have same band gap). The lattice of CPCs is arranged in concentric layers. The isotropic photonic band gap is originated from its high symmetry in the wave vector (k) space and has been verified by experiment [8]. After the CPC structure was proposed, many applications based on the structure have been rapidly developed. CPC high-Q microcavities [10], CPC resonators [11] and CPC microcavity lasers [12] have been reported recently. Other types of CPC cavities and resonators [13–16] also have been intensively studied and designed to achieve high Q factor. However, broadening of the band gap has never been discussed.

In this paper, different from the previously reported works, we present a new type of CPC structure to realize a broad and isotropic band gap. We used the idea of geometrical distribution of periods, which warrants substantial enlargement of omni-directional band gaps in 1D PC structure [7], to design CPC. The CPC is designed such that the distance between each concentric layer is geometrically distributed. We found that such a geometrically distributed CPC possess a very broad and isotropic band gap compared to an ordinary CPC.

The origination of the isotropic of band gap of GCPC is owing to the arbitrary rotational symmetry of the structure the same as the CPC structure which has been verified by changing the incident angle of a millimeter wave [8]. Because of this, we do not show detailed analysis on the relationship between band gap size and different incident angles.

The arrangement of the GCPC structure is shown in Fig. 1. On the same concentric layer, the distance between any two rods is a

* Corresponding author.

E-mail addresses: gandhi@ihpc.a-star.edu.sg (G. Alagappan), echkam@ntu.edu.sg (C.H. Kam), exwsun@ntu.edu.sg (X.W. Sun).

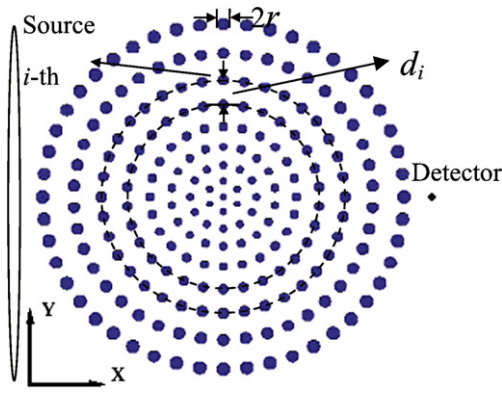


Fig. 1. The structure of GCPC. The black dot is the point detector used to collect information for DFT. The ellipse in the left side of the structure is the launched Gaussian wave.

constant and all rods are the same in size. The positions of the rods in the x - y plane (Fig. 1) are given by: [8]

$$\begin{aligned} x_i &= \sin\left(\frac{2m\pi}{6i}\right) \sum_1^i d_i, \\ y_i &= \cos\left(\frac{2m\pi}{6i}\right) \sum_1^i d_i \end{aligned} \quad (1)$$

In Eq. (1), d_i ($i = 1, 2, \dots, N$) is the distance between the $(i-1)$ th and i -th concentric layer (i.e., a circular layer indicated as dark dashed circle in Fig. 1), m is an integer ranging from 1 to $6i$, N is the total number of concentric layers. The radius of the rods, r_i , and the distance between each concentric layer, d_i , are geometrically distributed with the ratio, r_i/d_i , as a constant. The expression for d_i is $d_i = d_0 R^{(i-1)}$, ($i = 1, \dots, N$), where R and d_0 represent the common ratio of the geometrical progression and the smallest distance between the concentric layers, respectively. The radius of the central rod, r_0 , is equal to r_1 .

The modeling approach used in this paper is based on the finite difference time domain (FDTD) method, which is commonly applied in PC simulations [17,18]. For our FDTD computation, the input source is a pulsed Gaussian wave given by [17],

$$E(x) = A \cdot \exp\left[-\frac{1}{2}\left(\frac{x-x_0}{2T}\right)^2\right] \cdot \exp\left[-\frac{1}{2}\left(\frac{t-t_{off}}{t_0}\right)^2\right] \quad (2)$$

where A , x_0 , T , t_{off} , t_0 represent field amplitude, center position, half width, time offset and pulse width, respectively. A desired range of frequency (or wavelength) can be obtained by appropriately controlling the time pulse. The frequency spectrum is obtained by using a discrete Fourier Transform (DFT) method [19]. All these parameters (A , x_0 , T , t_{off} , t_0) must be carefully optimized to make sure that the DFT of the time pulse is large enough to cover the desired band edges. The Gaussian beam is launched along the x -direction from the left side at the middle of vertical direction of the structure (see Fig. 1). A point detector, which is placed in the other side of the structure opposite to the Gaussian beam, is used to collect information needed for the DFT. The point detector is indicated as a black dot in Fig. 1.

In Fig. 2, we present spectra for two different CPC designs. In this figure, the horizontal axis is the wavelength and the vertical axis is the transmittance at the detector. The two structures are constructed as follows: The uniform CPC structure is constructed with $d_i = d_0$ and $r_i = r_0$ for the whole structure, $r_i/d_i = r_0/d_0 = 0.2$, ($i = 1, 2, \dots, N$). The GCPC structure is constructed with the rules of $d_i = d_0 R^{(i-1)}$ ($i = 1, 2, \dots, N$) and $r_i/d_i = 0.2$. All the parameters are chosen as follows: $d_0 = 0.4096 \mu\text{m}$, $r_0/d_0 = 0.2$, $R = 1.1$, $N = 10$, $r_0 = r_1$, for both uniform CPC and GCPC. The refractive index of the rod is 3.6, which is the same as silicon and the ambient medium is taken as air. The common ratio, R , has the same

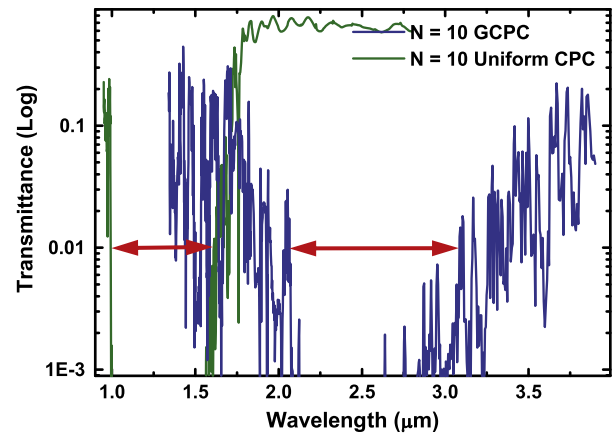


Fig. 2. The spectra of different CPC designs. The green solid line represents the spectrum of uniform CPC with $d_i = d_0$ and $r_i = r_0$ for the whole structure. The blue solid line represents the spectrum of the GCPC constructed with the rule of $d_i = d_0 R^{(i-1)}$. Here $d_0 = 0.4096 \mu\text{m}$, $r_0/d_0 = 0.2$, $N = 10$, $R = 1.1$, $r_i/d_i = 0.2$ for both uniform CPC and GCPC. The refractive index of the rods is 3.6.

meaning as in the 1D case [7], but the value of R here is smaller than that in 1D case. In 1D case, each component of the whole geometrically distributed structure is a 1D PC, which means each component has its own band gap, so R can be set larger [7]. For the 2D case, the GCPC is constructed by using of concentric layers of rods which do not have their own band gap. In this case, common ratio, R , should be chosen to be a relatively small value to make sure that the whole GCPC can form a band gap.

The green solid line in Fig. 2 represents the transmission spectrum of the uniform CPC. On the other hand, the blue solid line indicates the transmission spectrum of the GCPC. The upper and lower band edges are defined as the end points of the wavelength range where the transmittance is below 0.01. The band gaps of CPC and GCPC are identified with red arrows in Fig. 2. From the figure, it is clear that the GCPC has a broader band gap than the uniform CPC. The band gap sizes of the uniform CPC and the GCPC are $0.619 \mu\text{m}$ and $1.42 \mu\text{m}$, respectively. The band gap of the GCPC has been enlarged about 130% compared to the uniform CPC. The lower band edge of the GCPC in Fig. 2 seems to be red-shifted in comparison to the uniform CPC. Detailed discussion of the red-shift of the band gap will be given in the following paragraphs. Here it is worth pointing out that there are also some small peaks in the band gap of the GCPC. These small peaks can be suppressed by increasing the refractive index of the rods. This can be easily understood from the properties of photonic crystals. The larger the contrast of the refractive index of two different materials is, the flatter the band gap of the photonic crystals is.

To investigate the origin of the red shift in the transmission spectrum of the GCPC, the relationship of band gap width and the number of the concentric layers of GCPC is studied. Fig. 3 shows the band edges of the GCPC as a function of the number of concentric layers (N). The upper and lower band edges are defined using the same criterion used to define the band edges in Fig. 2. The red dashed line indicates the upper band edge of the band gap of the GCPC for different number of concentric layers. On the other hand, the black solid line indicates the lower band edge of the band gap of the GCPC. All of the design parameters used for Fig. 3 are the same as those in Fig. 2 except for N . From Fig. 3, we can clearly see the broadening and red-shifting of the band gap with the increasing number of the concentric layers. For GCPC, both of the band edges almost linearly increase with the upper band edge increasing faster than the lower band edge. There could be several reasons for the red shift of the band gap. Firstly, the effective refractive index of the GCPC increases with the increasing number of the concentric layers. The rods become larger and occupy more spaces in the structure, which then causes the

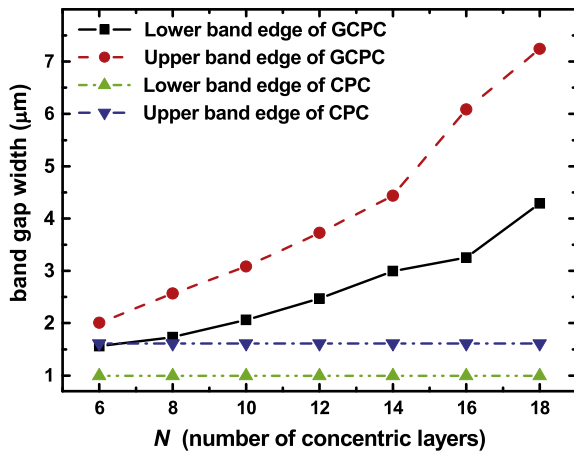


Fig. 3. The band gap width versus the number of concentric layers of GCPC and uniform CPC respectively.

effective refractive index of the GCPC to be larger. This increase in the effective refractive index causes the red shifts of the band edges in the GCPC. Secondly, the red shift of band gap may come from the blocking of the inner concentric layers. When the electromagnetic wave is blocked by the inner concentric layers, the electromagnetic wave may not be totally reflected back but propagates to the rear of the GCPC in the outer concentric layers and is collected by the point detector that is placed in the right side of the structure. In Fig. 3, we also plot the band gap width of uniform CPC with $d_i = 0.4096 \mu\text{m}$, as a function of the number of concentric layers. The uniform CPC used here is the same as the uniform CPC used in Fig. 2. The blue (dash-dotted) line indicates the upper band edge of the band gap of the uniform CPC for various N , and the green (dash-dot-dot) line indicates the lower band edge of the band gap of the uniform CPC. It is clear that the width of the band gap is almost the same despite the increasing number of

concentric layers. From the above study, we can conclude that the broadening of isotropic band gap can be obtained using GCPC simply by increasing the numbers of the concentric layers.

In summary, the optical properties of a new type, aperiodic, two-dimensional GCPC have been studied. Broad and isotropic band gap has been achieved by increasing the number of concentric layers. The red shift of the band gap is attributed to two reasons: (1) the increase of the effective refractive index, and (2) the light blockage by the inner part and propagation by the outer part of the GCPC. The GCPC can be used to achieve broad and isotropic band gap by only increasing the number of concentric layers in a common ratio (R), which is an easy way to design a broad band gap optical device.

References

- [1] E. Yablonovitch, *Physical Review Letters* 58 (1987) 2059.
- [2] S. John, *Physical Review Letters* 58 (1987) 2486.
- [3] S.J. McNab, N. Moll, Y.A. Vlasov, *Optics Express* 11 (2003) 2927.
- [4] O. Painter, R.K. Lee, A. Scherer, A. Yariv, J.D. O'Brien, P.D. Dapkus, I. Kim, *Science* 284 (1999) 1819.
- [5] Y. Akahane, T. Asano, B.S. Song, S. Noda, *Nature* 425 (2003) 944.
- [6] Q.G. Du, F.F. Ren, C.H. Kam, X.W. Sun, *Optics Express* 17 (2009) 6682.
- [7] G. Alagappan, P. Wu, *Optics Express* 17 (2009) 11550.
- [8] N. Horiuchi, Y. Segawa, T. Nozokido, K. Mizuno, H. Miyazaki, *Optics Letters* 29 (2004) 1084.
- [9] J. Zarbakhsh, F. Haggmann, S.F. Mingaleev, K. Busch, K. Hingerl, *Applied Physics Letters* 84 (2004) 4687.
- [10] S.S. Xiao, M. Qiu, 6th International Symposium on Photonic and Electromagnetic Crystal Structures (PECS-VI), Aghia Pelaghia, Greece, 2005, pp. 134–138.
- [11] J. Scheuer, A. Yariv, *Physical Review E* 70 (2004) 036603.
- [12] P.T. Lee, T.W. Lu, J.H. Fan, F.M. Tsai, *Applied Physics Letters* 90 (2007) 151125.
- [13] D. Chang, J. Scheuer, A. Yariv, *Optics Express* 13 (2005) 9272.
- [14] J. Vuckovic, M. Loncar, H. Mabuchi, A. Scherer, *Ieee Journal of Quantum Electronics* 38 (2002) 850.
- [15] J. Scheuer, A. Yariv, *Ieee Journal of Quantum Electronics* 39 (2003) 1555.
- [16] H.Y. Ryu, M. Notomi, G.H. Kim, Y.H. Lee, *Optics Express* 12 (2004) 1708.
- [17] A. Taflove, S.C. Hagness, *Computational Electrodynamics: The Finite-Difference Time-Domain Method*, Artech House, 2000.
- [18] Y.T. Fang, J. Zhou, *Journal of Russian Laser Research* 28 (2007) 372.
- [19] Smith, S.W., *The Scientist and Engineer's Guide to Digital Signal Processing*, California Technical Publishing, 1999.